DEVICES

The missing link: Unlocking the power of cardiac rhythm monitoring device based QT interval detection

Antony F. Chu MD, FHRS[1] (iD) | **Gautham Rajagopal MS**[2] (iD) | **Shantanu Sarkar PhD**[2]

[1] Warren Alpert School of Medicine, Brown University, Rhode Island Hospital, 593 Eddy St, APC Building, Division of Cardiology, Providence, Rhode Island, USA

[2] Medtronic Inc, 8200 Coral Sea St. Mounds View, Mounds View, Minnesota, USA

Correspondence
Antony F. Chu, MD, FHRS, Warren Alpert School of Medicine, Brown University, Rhode Island Hospital, 593 Eddy St, APC Building, Division of Cardiology, Providence, RI 02903, USA.
Email: antony_chu@brown.edu

[Correction added on Aug 2, 2022, after first online publication: The copyright line was changed.]

Abstract

Background: The QT interval is of high clinical value as QT prolongation can lead to Torsades de Pointes (TdP) and sudden cardiac death. Insertable cardiac monitors (ICMs) have the capability of detecting both absolute and relative changes in QT interval. In order to determine feasibility for long-term ICM based QT detection, we developed and validated an algorithm for continuous long-term QT monitoring in patients with ICM.

Methods: The QT detection algorithm, intended for use in ICMs, is designed to detect T-waves and determine the beat-to-beat QT and QTc intervals. The algorithm was developed and validated using real-world ICM data. The performance of the algorithm was evaluated by comparing the algorithm detected QT interval with the manually annotated QT interval using Pearson's correlation coefficient and Bland Altman plot.

Results: The QT detection algorithm was developed using 144 ICM ECG episodes from 46 patients and obtained a Pearson's coefficient of 0.89. The validation data set consisted of 136 ICM recorded ECG segments from 76 patients with unexplained syncope and 104 ICM recorded nightly ECG segments from 10 patients with diabetes and Long QT syndrome. The QT estimated by the algorithm was highly correlated with the truth data with a Pearson's coefficient of 0.93 (p < .001), with the mean difference between annotated and algorithm computed QT intervals of −7 ms.

Conclusions: Long-term monitoring of QT intervals using ICM is feasible. Proof of concept development and validation of an ICM QT algorithm reveals a high degree of accuracy between algorithm and manually derived QT intervals.

KEYWORDS
insertable cardiac monitor, long-term cardiac monitoring, QT interval, QTc interval

1 | INTRODUCTION

The QT interval measured on the 12-lead electrocardiogram (ECG) is clinically important as prolongation of this interval correlates with abnormalities in cardiac ventricular repolarization and can precede potentially fatal ventricular cardiac arrhythmias such as polymorphic ventricular tachycardia, Torsades de Pointes (TdP) and sudden cardiac death.[1–3] In the clinical setting, measurements of the QT interval is subject to substantial variability, leading to disparities in interpretation. This variability in QT interval measurement results from biological factors, such as diurnal effects, electrolyte variance,

---

Abbreviations: AF, Atrial Fibrillation; ICM, Insertable cardiac monitor; PVC, Premature ventricular complex or contraction; TdP, Torsades de pointes

medications and technical considerations including: environmental high-frequency noise, signal processing and the variance in signal acquisition of the electrogram recording. In addition, there is a lack of consensus among experts regarding standardizing approaches to measure the QT interval (based on heart rate and arrhythmia) which results in statistical variance.[2,4–5]

Factors leading to QT prolongation and TdP are multi-factorial. Among these, an important risk factor for prolongation of the QT interval is the drug-drug interactions and the use of QT prolonging drugs.[6–7] A QT interval greater than 500 ms has been shown to correlate with a statistically significant higher risk of TdP.[2] Given the clinical importance of accurately measuring the QT interval, we sought to develop and validate a proof-of-concept QT detection algorithm for continuous monitoring of QT interval in patients receiving an Insertable Cardiac Monitor (ICM).

2 | METHODS

2.1 | Algorithm design

The QT detection algorithm is designed to detect T-waves and determine the QT interval for every ventricular beat in an ICM. Figure 1 shows the general schematic of the 5-step QT detection algorithm: (1) The ICM electrogram signal is band filtered and rectified. The R-waves are sensed by using a dual channel sensing scheme. (2) The R-wave peaks are determined in the rectified signal based on the R-wave sensing and RR intervals are computed. (3) Based on the RR interval, QT algorithm parameters are computed to define a search window after the QRS complex. (4) The T-wave location is determined by the algorithm within the defined search window. (5) Based on the T-wave location, QT interval and QTc intervals are computed for every ventricular beat.

The R-waves are sensed using a dual channel sensing scheme. A secondary sensing channel was used in addition to the primary sensing channel to reduce under sensing of ventricular beats such as premature ventricular complexes (PVCs).[8] To distinctly identify the T-wave signal, the electrogram signal is filtered, using a pass band filter of 6 to 20 Hz to enhance T-waves, and then rectified. To detect the T-wave location, the algorithm calculates a T-wave search window following the QRS complex. The duration of the search window is determined based on both the current RR interval and the RR interval of the previous ventricular beat. For instance, if the previous RR interval is shorter, then the search window following the current QRS complex will also be shorter. The search window is functionally designed to optimize T-wave detection in the time period following the inscription of the QRS complex and preceding the onset of the P-wave of the subsequent beat. The parameters used to define the search window are determined using data analytic optimization techniques for RR intervals ranging from 300 to 1400 ms.

Panel A in Figure 1 shows the various parameters computed by the QT detection algorithm to determine the search window based on both the previous and current RR intervals. Initially, the start and end for the search window is determined based on the previous RR interval. If the

end of the search window is very close to the R-wave of the next beat, then the end of the search window is determined based on the current RR interval instead to end the search window prior to the P-wave. In addition, if the current RR interval is greater than the previous RR interval by 500 ms or the previous beat was determined to be distorted by artifact, then the algorithm determines the search window parameters based on the current RR interval. Panel B in Figure 1 shows an example of an ICM electrogram signal and the corresponding filtered and rectified waveform. The dotted green lines depict the start and end of the search window for each beat as calculated by the algorithm. The solid blue lines depict the locations of the algorithm-detected T-waves for each beat within the search window.

The sample with the maximum 9-sample median value of the electrogram within the search window is selected by the algorithm as the T-wave location enabling it to compute the QT interval. Functionally, the algorithm looks for the sample on the ICM electrogram with the highest slew rate in the T-wave and selects this as the correct location of the T-wave. The Framingham (linear correction formula) and Bazett formulas were used for calculation of the corrected QT interval (QTc).[9,10] The QTc intervals is computed using the Framingham's formula[11,12] as:

$$QTc = QT + 0.154 (1 - RR)$$

The QTc intervals is computed using the Bazett formula as:

$$QTc = QT / \sqrt{RR}$$

2.2 | Data and statistical analysis

The QT detection algorithm was developed using automatically detected episodes by the Reveal XT ICM device in real world patients. Two different data sets (independent from the development data set) were used to validate the QT detection algorithm. The algorithm was validated using: (1) nightly transmitted 10 s ICM electrogram transmissions from patients with diabetes and Long QT syndrome and (2) 30 s ICM electrogram transmissions from patient activated episodes from patients implanted with a Reveal LINQ ICM for unexplained syncope indication in the month of March of 2014. Real world data from ICM patients were used from the de-identified Medtronic CareLink data warehouse. All patients in the de-identified Medtronic CareLink data warehouse provided consent to use of their device data for research purposes. The determination of diabetes and Long QT syndrome was obtained using ICD9/ICD10 diagnostic codes from a merged database of de-identified Optum electronic health record database with the Medtronic CareLink data warehouse. Selection of patients from a real-world data set provided variable T-wave morphologies reflecting dynamic changes in T-wave sensing due to varying patient posture (e.g., lying/standing/sitting) over time. The manufacturer's recommended anatomical location for the ICMs is placement at the 4th intercostal space at 45 degrees or vertical orientation.

The episodes in the development and validation data sets were randomly selected to ensure that the data set was representative of real-world differences. Both the data sets were randomly chosen even before the designing process began for the development
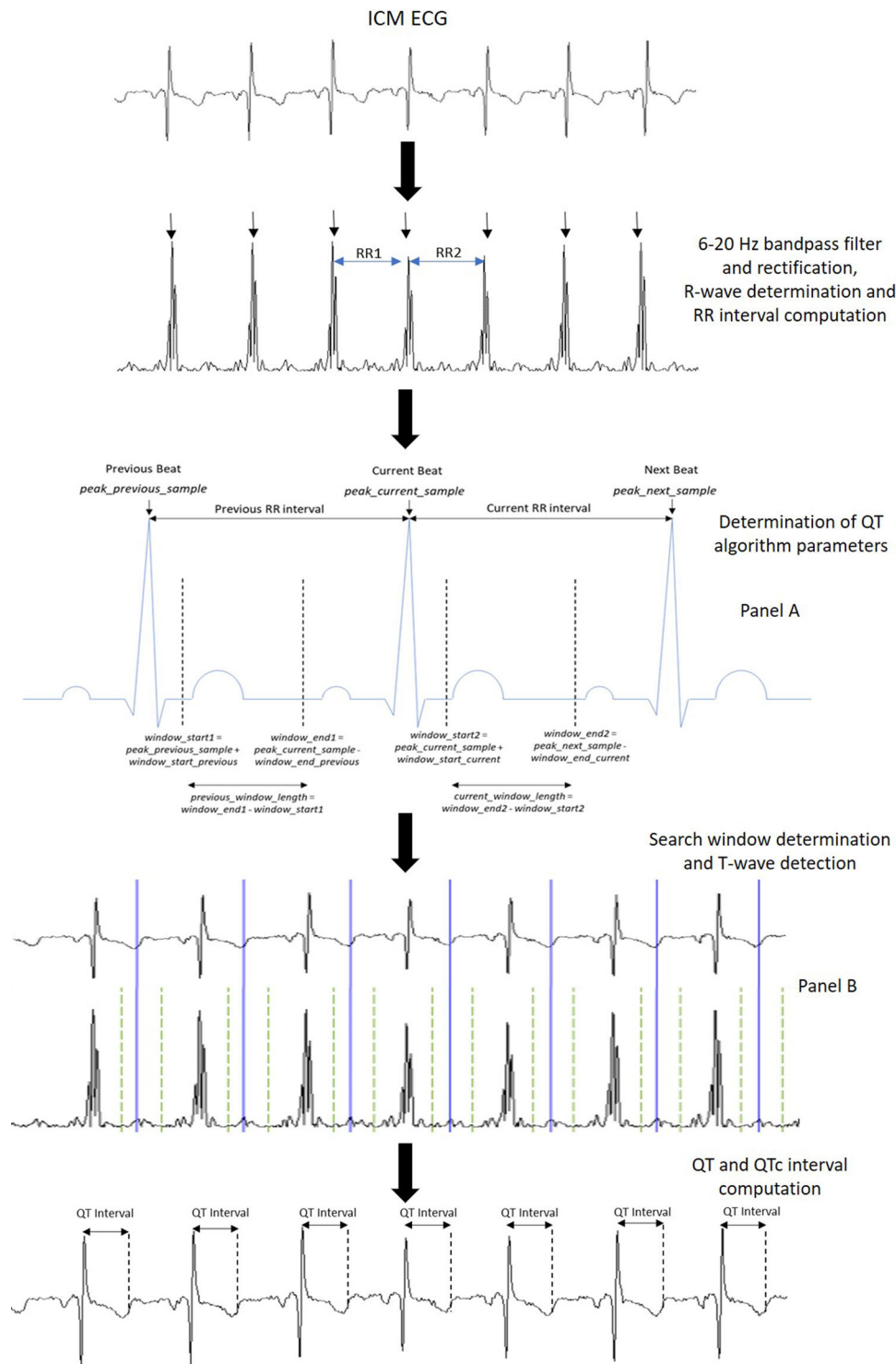
FIGURE 1   General schematic of the QT detection algorithm [Color figure can be viewed at wileyonlinelibrary.com]

of the QT algorithm to ensure that there was no bias in the selection of the data. The data set included representation of normal sinus rhythms, both tachycardia and bradycardia events, and other cardiac arrhythmias (e.g., Atrial Fibrillation [AF], PVCs) to validate the QT algorithm performance over a spectrum of heart rates and assess QT interval precision irrespective of the RR interval. Moreover, the data sets included nightly transmission as well as patient activated episodes to ensure that the ICM algorithm accurately detects T-waves during both the day and night when the patient is assuming different physical positions (standing/sitting/lying) and thus influencing T-wave morphology.

For both data sets, manual annotations to detect T-waves were performed by a single reviewer who was blinded to device detections with a confirmation review performed by a second blinded reviewer for difficult cases. Annotations were assigned to distinguish between normal beats and signals distorted by baseline artifact. Distorted signals

as determined by manual annotation are excluded from the QT analysis. The QT intervals obtained from the QT detection algorithm was compared to the QT interval computed from manually annotated T-waves to evaluate the performance of the algorithm. A 12-beat median of QT intervals was considered for evaluating the performance. To evaluate the interobserver variability in the manual QT annotations, adjudication of all ICM electrograms in the validation dataset were performed by two independent reviewers who were blinded to device detections. The interobserver variability was computed as the average of the difference between the QT annotations of both the reviewers.

The performance of the QT detection algorithm was evaluated by comparing QT intervals detected by the algorithm and QT from manual annotations using the Pearson's correlation coefficient and the Bland Altman plot. Pearson's correlation coefficient is a measure of the strength of a linear association between two variables. For the Bland-Altman plot, the differences between the two measurements were plotted against the averages of the two measurements. The upper and lower limits of agreements were computed as the mean difference ± 1.96 times the standard deviation of the differences.

To evaluate the correlation of QT intervals between surface ECG and corresponding ICM ECG, a separate dataset of 25 patients who had both ICM ECG and 2-lead surface ECG data available simultaneously was chosen.[13] A 60-s ICM and surface ECG snippet was randomly chosen from each patient for manual annotation. Manual annotations were performed to annotate QT intervals for every beat from both the LINQ ICM and surface ECG for all patients in this dataset. This dataset provided over 1500 beats for analysis from ICM ECG and surface ECG data. Performance was evaluated between (1) QT interval annotations from surface ECG and ICM ECG data, (2) QT interval annotations from surface ECG and algorithm detected QT intervals, and (3) QT annotations from ICM ECG and algorithm detected QT intervals. For all the three analysis, the performance was evaluated by determining the Pearson's correlation coefficient. The mean of the difference between the QT intervals between the two datasets was also computed as an additional performance metric.

3 | RESULTS

The QT detection algorithm was developed using 144 ICM ECG episodes from 46 patients which had T-waves with different morphologies. Figure 2A shows the correlation plot between the QT interval computed from manual annotations and QT interval computed from the algorithm results for the ICM ECG development data set. The QT estimated by the algorithm from the ICM ECG data set correlated with the annotated QT intervals with a Pearson's correlation coefficient of 0.89 (p value <.001). Figure 2B depicts the Bland-Altman plot for the ICM ECG development data set.

The validation data set consisted of 104 nightly ECG episodes (each 10 s) stored in LINQ devices from patients with diabetes and Long QT syndrome and 136 patient activated episodes (30 s ECG snippets) from patients implanted with an ICM for unexplained syncope indication. The validation data set had over 6200 beats from 86 patients for

analysis. The data set with patient activated episodes consisted of 76 patients with ICM implanted for unexplained syncope. The mean age at implant was 66 years. Gender information was available in only 19 of the 76 patients with eight of 19 patients in this data set were identified as male. The data set with nightly transmitted episodes consisted of 10 patients with ICM with a mean age of implant of 65 years. All 10 patients had Long QT syndrome and type two diabetes. The primary indication for ICM implant was unexplained syncope for five patients. Two patients were implanted for AF Ablation monitoring and Cryptogenic stroke, Suspected AF and Ventricular tachycardia were the reason for ICM implant in the remaining three patients.

Figure 2C shows the correlation plot between the QT interval computed from manual annotations and QT interval computed from the algorithm results for the ICM ECG validation data set. The QT estimated by the algorithm from the ICM ECG data set were highly correlated with the manually annotated QT intervals with a Pearson's correlation coefficient of 0.93 (p value <.001). Figure 2D depicts the Bland-Altman plot for the ICM ECG validation data set. The mean of the difference between manually annotated and algorithm computed QT intervals was −7 ms and the lower and upper limits of agreement were −38 and 23 ms respectively. A mean of bias of −7 ms shows that the algorithm detected QT, on an average, overestimates the manually annotated QT by 7 ms. This overestimate may be due to difference in the method of T-wave detection. The manual annotation method detects the peak amplitude of the T-wave whereas the algorithm detects the highest slew of the T-wave. T-wave detection utilizing the slew rate method generally places the T-wave location slightly later compared to the peak amplitude of the T-wave. Since the ICM electrogram data is sampled at 256 Hz, the sampling resolution of the ICM signal is approximately 4 ms. Additionally, the QTc intervals were computed using both Bazett and Framingham rate correction formulas. The QTc estimated by the algorithm from the ICM ECG data set using the Bazett and Framingham formulas correlated with the manually annotated QT intervals with a Pearson's correlation coefficient of 0.92 and 0.90 (p value <.001) respectively. The mean of the difference between manually annotated and algorithm computed QTc intervals using Bazett and Framingham formulas were −8.5 and −7.3 ms respectively.

Figure 3 shows examples in which the QT algorithm was able to accurately detect different types of T-waves with different phasic orientations, morphologies (Figures 3A and B) and poor T-wave signal Figure 3C, and in presence of rapid and variable heart rates Figures 3D–F). These examples also include variable RR intervals. By optimizing the search window duration for RR interval, the algorithm was able to adapt to dynamic beat-to-beat RR interval variations and accurately detect T-waves for varying RR intervals while avoiding detection of the P-wave as the T-wave. Specifically, Figures 3E and 3F shows examples of episodes with AF where T-waves are accurately detected despite beat-to-beat changes in the RR intervals. Figure 3G and 3H shows prototypical ICM electrogram transmission for which the difference between the annotated QT intervals and the QT estimated by the algorithm was greater than 25 ms, thus overestimating the QT interval compared to the manual annotation. In several of these events, the
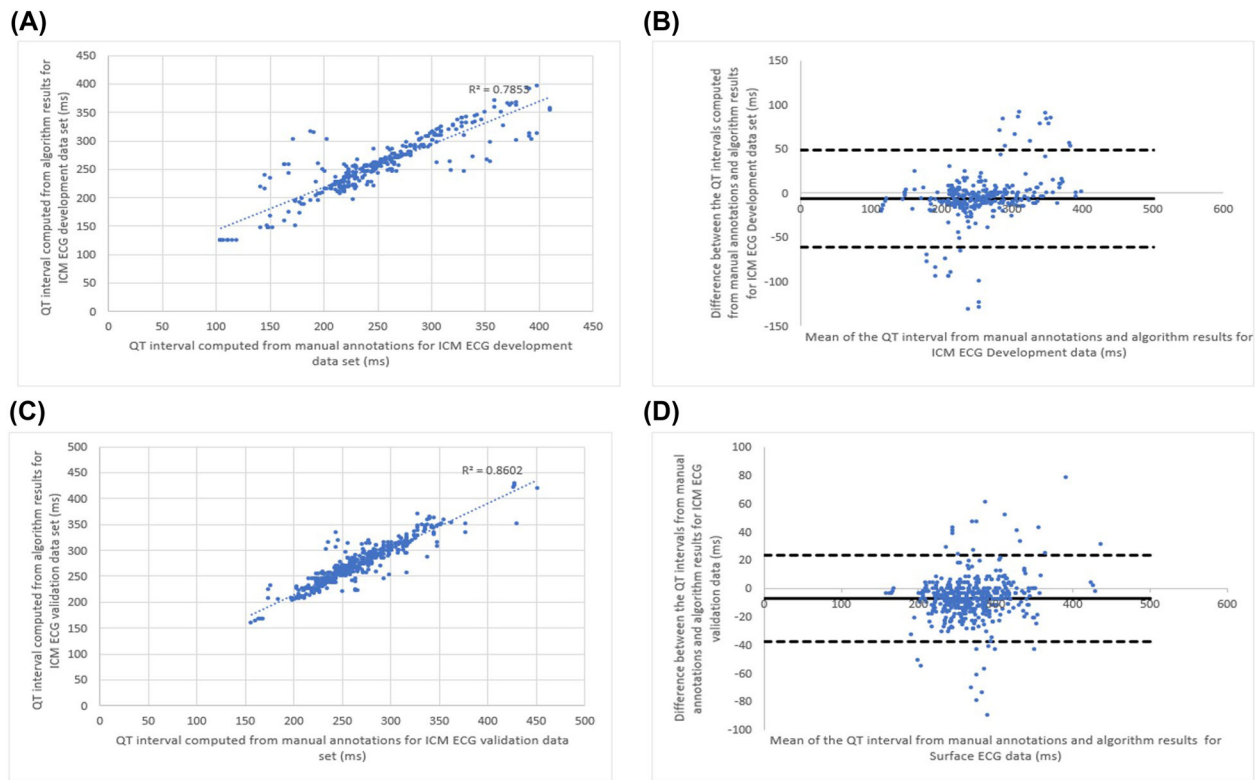
(A)

(B)

(C)

(D)

FIGURE 2 (a) Correlation plot between the QT interval computed from manual annotations and QT interval computed from algorithm results for ICM ECG development data set. (b) Bland Altman plot for the ICM ECG development data set. (c) Correlation plot between the QT interval computed from manual annotations and QT interval computed from algorithm results for ICM ECG validation data set. (d) Bland Altman plot for the ICM ECG validation data set [Color figure can be viewed at wileyonlinelibrary.com]

algorithm detected the T-wave in a different location when compared to the manual annotation, however the algorithm determined T-wave location is noted to be consistently shorter or longer. Thus, relative changes in QT interval can still be measured in these cases even though the difference is comparatively larger in these files. There were some outlier cases where the difference between annotated and algorithm detected QT intervals were more than 75 ms with the reason for these cases being small T-waves and presence of noise around the detected T-wave.

To further evaluate the performance of the algorithm when measuring QT interval in patients with AF, the algorithm was evaluated separately on patient files which were identified to have AF or atrial tachycardia. In the seven episodes from six patients which had AF, the QT estimated by the algorithm correlated with the annotated QT intervals with a Pearson's correlation coefficient of 0.92. The mean of the difference between manually annotated and algorithm computed QT intervals was −9.3 ms in this data set with AF. The results in patients with AF were very similar compared to the overall results.

Example of a long-term monitoring QT trend that an ICM could provide is shown in Figure 4. Figure 4A shows the QTc detected by the algorithm over 714 days using 10 s ICM electrograms transmitted nightly from a patient with implanted ICM with both diabetes and Long QT syndrome. The 10-day moving average QTc intervals show a lot of day-to-

day variability. Figure 4B shows an example of another patient from the same data set with 313 nightly transmitted episodes with the 10-day moving average QTc intervals showing lesser variability. In an actual implementation, QT intervals can be estimated using all beats during a day and aggregated QT intervals can be generated for different time periods during the day. The interobserver variability was found to be 4.38 ms which was computed as the average of the difference between the QT annotations performed for every beat in the validation dataset by two independent reviewers which revealed good interobserver agreement. The sampling rate of the ICM ECG signal which was used for annotation was 256 Hz thus providing 3.9 ms as the resolution of the QT measurements.

On the separate dataset with 25 patients with both ICM ECG and 2-lead surface ECG data available simultaneously, the manually annotated QT intervals computed from surface ECG were highly correlated with the corresponding manually annotated QT intervals from ICM ECG with a Pearson's correlation coefficient of 0.85 (p value <.001). It was often easier to annotate QT intervals in ICM ECG compared to surface ECG. The mean of the difference between manually annotated surface ECG and ICM ECG QT intervals was found to be 6.3 ms. The QT intervals detected by the algorithm were found to be highly correlated with the corresponding manually annotated QT intervals from ICM ECG (Pearson's correlation coefficient of 0.96, p <.001; mean difference of 7.4 ms) as well as manually annotated QT intervals from
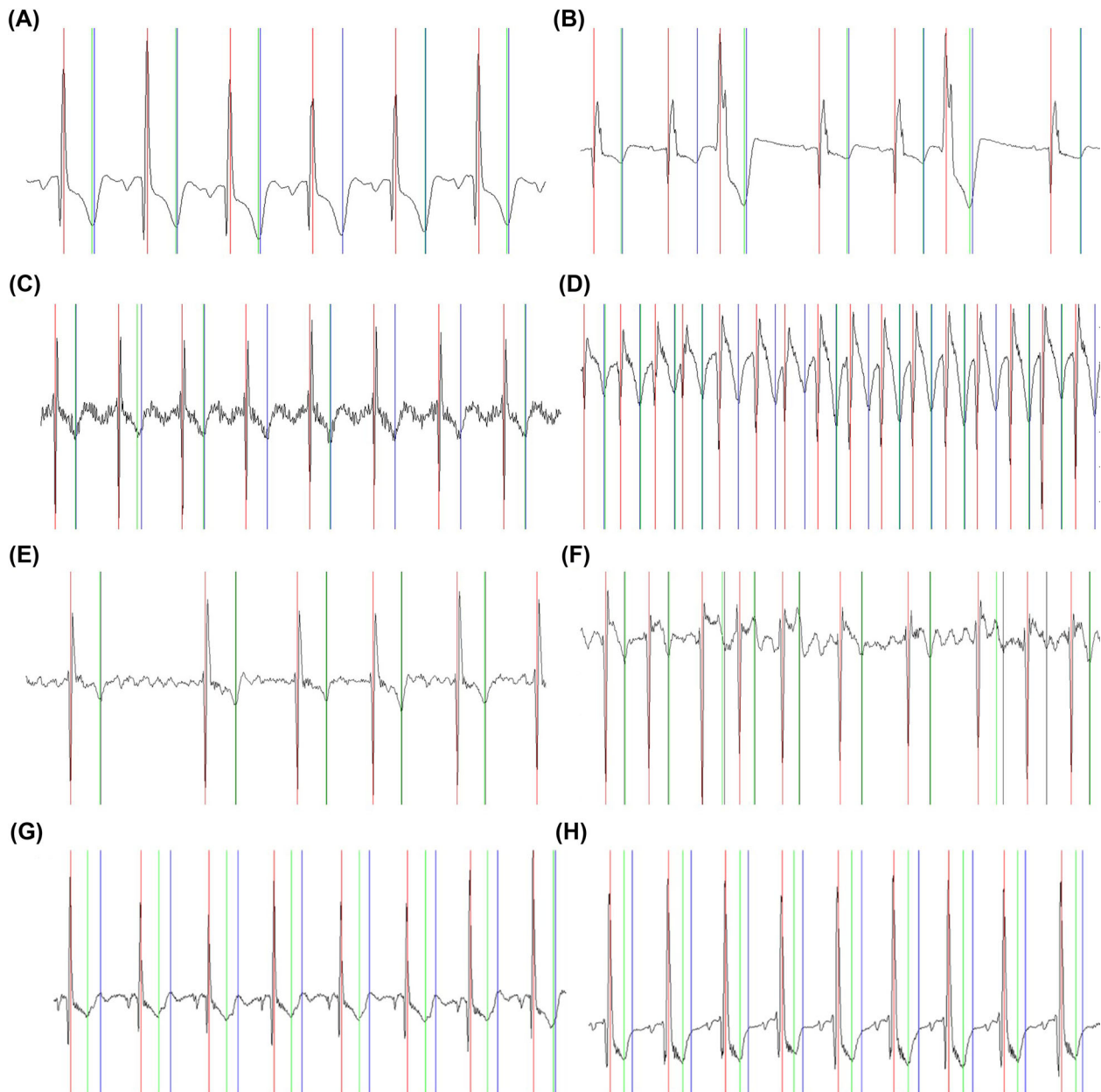
FIGURE 3 Examples of ECG strips from the development and validation data set depicting T-waves with different morphologies and orientations at different RR intervals with both manual annotations and the corresponding algorithm detections. The red markers depict the device detected R-wave markers. The green markers depict the T-wave location as determined from manual annotation and the blue markers depicts the T-wave location as determined by the QT detection algorithm [Color figure can be viewed at wileyonlinelibrary.com]

surface ECG (Pearson's correlation coefficient of 0.71, p <.001; mean difference of 16.3 ms).

4 | DISCUSSION

The study is aimed at developing and validating a proof-of-concept algorithm for continuous long-term derivation of QT intervals using an ICM. The Pearson's correlation coefficient of 0.93 between the QT estimated by the algorithm and the manually annotated QT intervals shows a statistically high correlation. The development and validation

data sets were chosen in such a way to include several different types of T-waves at different morphologies and orientation to ensure that the algorithm can detect these T-waves. In addition to this, the data set included both nightly transmitted ICM electrograms and daytime patient activated ICM electrograms ensuring that the algorithm can detect T-waves accurately during both daytime and nighttime. The high correlation coefficient shows that the algorithm is capable of detecting both short- and long-term QT variations accurately. These data may ultimately impact decision in clinical management as QT variation occurs with dynamic changes in physiologic conditions, metabolism, and dosing of medications such as insulin and antiarrhythmic drugs.
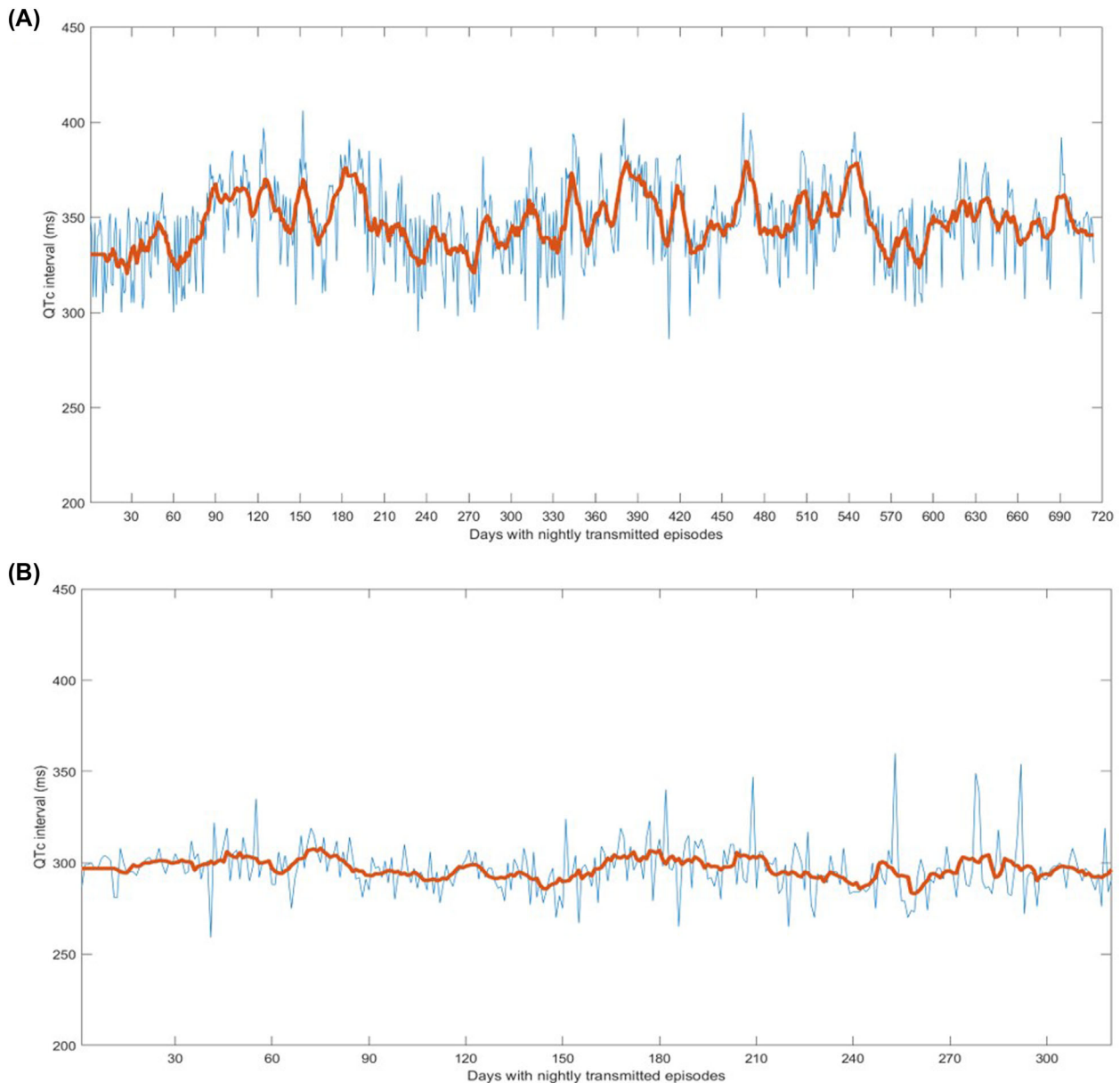
(A)

(B)

FIGURE 4 Examples of long-term monitoring QTc trend in a patient with (a) 714 nightly transmitted ICM ECG episodes. (b) 313 nightly transmitted ICM ECG episodes. The red plot depicts the 10-day moving average QTc interval [Color figure can be viewed at wileyonlinelibrary.com]

The QT detection algorithm defined in this study represents an innovative first-generation diagnostic for QT monitoring. Our study represents, to our knowledge, the first proof-of-concept demonstration of T-wave detection using an ICM algorithm. Additional enhancements and validation of the algorithm are on-going and reflect performance in real world patients. Enhanced versions of the algorithm may include a robust noise detection feature to improve signal fidelity and minimize extraneous noise. Furthermore, a confidence level metric can also be computed in real-time to convey the level of confidence in the accuracy of the detected T-waves. Improving the sampling frequency of the ECG signal can also improve the accuracy of the QT interval estimated by the algorithm. Additionally, investigating T-wave duration and morphological alternans or other forms of repolarization abnormalities are being considered.

Presently, QT interval monitoring is performed manually in the hospital setting. There is no currently approved continuous long-term analysis available for QT interval monitoring. Under this current rubric, patients undergoing anti-arrhythmic medication dosing must be inpatient hospitalized for several days for QT interval monitoring. An ICM capable of monitoring QT continuously may help reduce such hospitalizations and can provide continuous QT and QTc trends to the physicians. Continuous QT interval ICM monitoring also promises to assist physicians in correlating QT changes with occurrences of cardiac arrhythmias and modifying the drug dosages accordingly to minimize toxic effects of drug induced QT interval prolongation. Monitoring changes in QT interval using an ICM can provide important information to physicians that can reflect real-time dynamic changes in physiologic states such as serum glucose and insulin. Clinical studies have noted

a correlation between QT changes, diabetes and cardiac death.[14–17] Acute hyperglycemia and hypoglycemia events have also been associated with significant increases of QTc and QTc dispersion, a predictor of arrhythmia risk and sudden death.[16,17]

QT monitoring using an ICM could also play an important role in obtaining drug approvals as assessment of QT prolongation and TdP is a key criterion for drug safety and approval. An ICM capable of long-term QT interval monitoring would provide invaluable information monitoring patients receiving novel drug treatment with known QT prolonging drugs as has been observed in the recent COVID-19 pandemic.

5 | LIMITATIONS

The primary limitation of the study was the relatively small size of the development and validation data sets. The ICM has the capability to monitor continuously for over 3 years of follow-up, thus the data presented for validation may not cover for all kinds of T-wave morphologies the QT algorithm may be subjected to in real-world use. For example, performance of the QT detection algorithm should be further evaluated when the underlying rhythm is AF or in subjects who have bundle branch block. Further, the QT algorithm is designed to detect the highest slew of the T-wave which is in between the peak and the end of the T-wave, and thus is different from how the QT interval is clinically computed which is till the end of the T-wave. But since the algorithm consistently detects the T-wave at the same location, it is still expected to capture relative variation in QT intervals. But the algorithm is expected to underestimate the QT interval compared to the clinically computed QT interval. The algorithm was developed and validated with ECG signals collected at 128 Hz and up sampled to 256 Hz, thus providing effective resolution of the measurement in the range from 4 to 8 ms. A higher resolution is ideal, however that will lead to higher battery drain in an ICM and hence is a limiting factor in the accuracy of the measurement. Also, comparing manually annotated points with the algorithm results and measuring results with a resolution of 4 to 8 ms could lead to discrepancies. Small variations in the location of manual annotation can lead to a 10 to 15 ms difference with the algorithm results. The QT annotation and testing was based on ECG measurement using a 4 cm dipole. Further investigations are required to evaluate differences between QT measurements determined by 12-lead surface ECG versus ICM electrograms.

6 | CONCLUSION

An algorithm for continuous long-term monitoring of QT intervals in an implantable cardiac monitor was developed and validated. The QT intervals detected by the algorithm were highly correlated with manually derived QT intervals. Continuous long-term monitoring of QT intervals is feasible using an implantable cardiac monitor.

AUTHOR CONTRIBUTIONS

Concept/Design: Antony F. Chu, Gautham Rajagopal, Shantanu Sarkar. Data analysis/interpretation: Antony F. Chu, Gautham Rajagopal, Shantanu Sarkar. Data collection: Gautham Rajagopal, Shantanu Sarkar. Drafting article: Antony F. Chu, Gautham Rajagopal, Shantanu Sarkar. Critical revision of article: Antony F. Chu, Gautham Rajagopal, Shantanu Sarkar. Approval of article: Antony F. Chu, Gautham Rajagopal, Shantanu Sarkar.

ORCID

Antony F. Chu MD, FHRS https://orcid.org/0000-0002-8143-207X
Gautham Rajagopal MS https://orcid.org/0000-0003-3083-5351

REFERENCES

1. Viskin S. Long QT syndromes and torsade de pointes. *Lancet* 1999;354(9190):1625–1633.
2. Al-Khatib SM, LaPointe NM, Kramer JM, Califf RM. What clinicians should know about the QT interval. *JAMA* 2003;289(16):2120–2127.
3. Cox, Natalie K. The QT interval: how long is too long?. Nurs. Made Incred. Easy. 2011;9(2):17–21.
4. Morganroth J, Brozovich FV, McDonald JT, Jacobs RA. Variability of the QT measurement in healthy men, with implications for selection of an abnormal QT value to predict drug toxicity and proarrhythmia. *Am J Cardiol* 1991;67(8):774–776.
5. Molnar J, Zhang F, Weiss J, Ehlert FA, Rosenthal JE. Diurnal pattern of QTc interval: how long is prolonged? Possible relation to circadian triggers of cardiovascular events. *J Am Coll Cardiol.* 1996;27(1):76–83.
6. Morganroth J, Shah RR, Scott JW. Evaluation and management of cardiac safety using the electrocardiogram in oncology clinical trials: focus on cardiac repolarization (QTc interval). *Clin Pharmacol Ther.* 2010;87(2):166–174.
7. Chouchoulis k, Chiladakis J, Koutsogiannis N, Davlouros P, Kaza M, Alexopoulos D. Impact of QT interval prolongation following antiarrhythmic drug therapy on left ventricular function. *Future Cardiol.* 2017;13(1):13–22.
8. Lustgarten DL, Rajagopal G, Reiland J, Koehler J, Sarkar S. Premature ventricular contraction detection for long-term monitoring in an implantable cardiac monitor. *Pacing Clin Electrophysiol.* 2020;43(5):462–470.
9. Postema PG, Wilde AA. The measurement of the QT interval. *Curr Cardiol Rev.* 2014;10(3):287–294.
10. Vandenberk B, Vandael E, Robyns T, et al. Which QT correction formulae to use for QT monitoring?. *J Am Heart Assoc.* 2016;5:1–10.
11. Luo S, Michler K, Johnston P, Macfarlane PW. A comparison of commonly used QT correction formulae: the effect of heart rate on the QTc of normal ECGs. *J Electrocardiol.* 2004;37:81–90.
12. Sagie A, Larson MG, Goldberg RJ, Bengtson JR, Levy D. An improved method for adjusting the QT interval for heart rate (the Framingham Heart Study). *Am J Cardiol.* 1992;70(7):797–801.

13. Sanders P, Pürerfellner H, Pokushalov E, et al. Performance of a new atrial fibrillation detection algorithm in a miniaturized insertable cardiac monitor: results from the Reveal LINQ Usability Study. *Heart Rhythm.* 2016;13(7):1425–1430.

14. Rossing P, Breum L, Major-Pedersen A, et al. Prolonged QTc interval predicts mortality in patients with type 1 diabetes mellitus. *Diabet Med.* 2001;18(3):199–205.

15. de Bruyne MC, Hoes AW, Kors JA, Hofman A, van Bemmel JH, Grobbee DE. QTc dispersion predicts cardiac mortality in the elderly: the Rotterdam Study. *Circulation* 1998;97(5):467–472.

16. Marfella R, Rossi F, Giugliano D. QTc dispersion, hyperglycemia, and hyperinsulinemia. *Circulation* 1999;100:25.

17. Lee SP, Yeoh L, Harris ND, et al. Influence of autonomic neuropathy on QTc interval lengthening during hypoglycemia in type 1 diabetes. *Diabetes.* 2004;53(6):1535–1542.